

Photoelectrical Phenomena and Current Kinetics in TlBr

Vaidotas KAŽUKAUSKAS^{1*}, Andrius JURGILAITIS¹, Juozas-Vidmantis VAITKUS¹,
Vladimir GOSTILO², Michail SHOROHOV²

¹Department of Semiconductor Physics and Institute of Materials Science and Applied Research Vilnius University, Saulėtekio 9, bldg.3, LT-10222 Vilnius, Lithuania

²Bruker Baltic, Ltd, Ganību dambis 26, P.O.Box 33, LV-1005, Riga, Latvia

Received 10 January 2008; accepted 01 March 2008

Photoelectrical and current transient properties of TlBr were investigated in the temperature region from -20°C up to $+20^{\circ}\text{C}$, in which the effect of ionic conductivity changes significantly. The thermal activation energy value of conductivity of about 0.78 eV could stand for several mechanisms, e.g., electronic and ionic conductivity. From the spectral dependencies of photocurrent several defect-related maxima in the region between 1 eV and 2.5 eV were identified, being dependent on sample prehistory, i. e., its excitation by light and/or voltage. The transient photocurrent kinetics have demonstrated a complex behaviour that could be explained by the combined influence of electron generation/recombination processes superimposed upon the effect of ionic conductivity. The results indicate that ionic conductivity can take place also at -20°C , though its influence is less because of the thermally activated character.

Keywords: TlBr, electronic and ionic conductivity, defects, carrier transport.

1. INTRODUCTION

Thallium bromide (TlBr) is an attractive and promising material for X- and γ -ray spectroscopy because of its wide bandgap (2.68 eV), high density (7.56 g/cm^3) and high atomic numbers (Tl: 81 and Br: 35) [1–3]. Such collection of the attractive properties ensure a high photon stopping efficiency. The pixellated TlBr gamma-rays detectors had demonstrated energy resolutions of 6.7 keV (5.5 %) FWHM and 22.3 keV (3.4 %) FWHM for 122 keV and 662 keV gamma-rays, respectively [2, 3]. Nevertheless one of the main problems still preventing it from the practical application is presence of the ionic conductivity, which sensitively depends on the temperature [4] and makes device characteristic unstable in time. It causes, e. g., degradation of spectroscopic performance because of the polarization phenomena if devices are operated at the room temperature [2].

2. SAMPLES AND EXPERIMENT

We have investigated photoelectrical and current transient properties of TlBr in the temperature region from -20°C up to $+20^{\circ}\text{C}$, in which the effect of ionic conductivity changes significantly [4]. Samples with dimensions of about $(4\times 3\times 1)\text{ mm}^3$ were provided with the evaporated gold contacts. Experiments were carried out in a four-stage Peltier cooler cryostat from Bruker Baltic Co. It enabled cooling down the samples by about 50°C from the reference temperature of the water supply. To enable optical excitation of the sample, an optical window was mounted into the cryostat. The current flowing through the sample was measured by a digital electrometric voltmeter Keithley 6517A. To investigate the photoelectrical spectral dependencies optical excitation of the sample by mono-

chromatic light from a Leitz monochromator was used. The monochromator was updated to ensure numerical control of the light wavelength and intensity. The temperature of the sample was controlled by a calibrated Si temperature sensor mounted into the cooler nearby the sample. Its resistivity was measured by a digital multimeter Fluke 45. All the data readout and experiment control were performed numerically from a PC via GPIB, RS-232 and LPT interfaces. In order to prevent the long-living sample polarization and its irreversible degradation, low applied electric fields of less than 150 V/cm were used. A number of experiments were carried out at the electric field strength over the sample as low as 3.8 V/cm (1.5 V). Nevertheless, because of the low signals and noise, series of measurements were repeated at 15, 30 and 60 V biases, giving the more informative results. The presented results were obtained at electric field strengths of about 150 V/cm.

3. RESULTS AND DISCUSSION

3.1. Current – Voltage (IV) characteristics

To test the contact properties, the IV curves were measured at different temperatures. They are presented in Fig. 1. It can be seen that the IV curves were symmetrical and linear in all cases, evidencing suitability of the used contacts. From these data we have evaluated sample resistance at 20°C being $R = 4.2\times 10^{10}\ \Omega$ and its conductivity of about $(3-4)\times 10^{10}\ \Omega^{-1}\text{ cm}^{-1}$.

Dependence of the conductivity on the temperature is presented in Fig. 2. Characteristically this dependence is not perfectly linear in Arrhenius plot, evidencing faster drop of the resistance at higher temperatures. This could be associated with the energy distribution of the states, from which carriers are generated [5]. On the other hand, this could be due to the simultaneous action of several conductivity mechanisms with different activation energies, e. g., electronic and ionic conductivity, with increasing influence

*Corresponding author. Tel.: +370-672-40208; fax.: +370-5-2366003.
E-mail address: vaidotas.kazukauskas@ff.vu.lt (V. Kazukauskas)

of the latter effect at higher temperatures. The evaluation of the thermal activation energy of this dependence gave us the approximate value of 0.78 eV that is very close to the value of 0.8 eV obtained by impedance spectroscopy at low frequencies in [6].

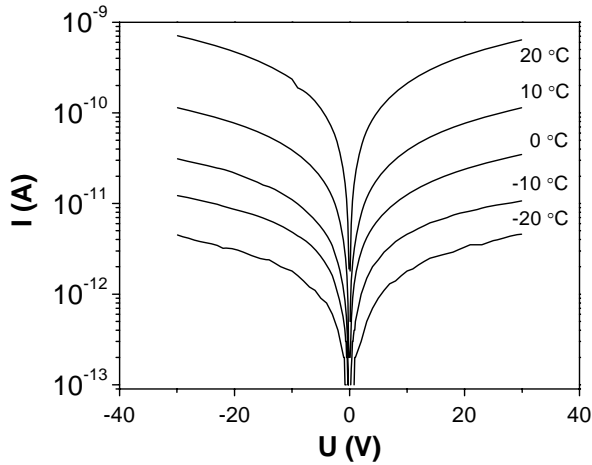


Fig. 1. Examples of the IV curves of the TlBr sample at different temperatures

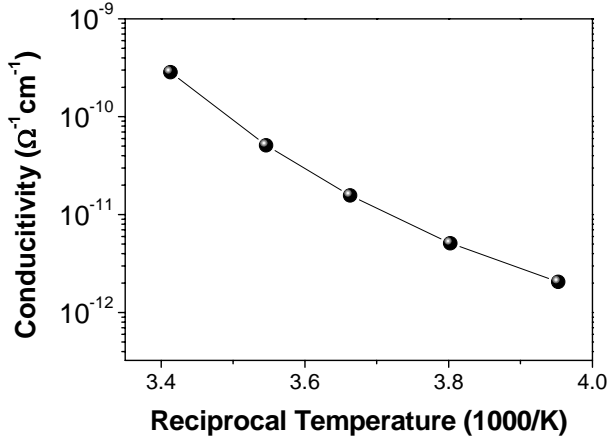


Fig. 2. Dependence of the sample conductivity on the reciprocal temperature

3.2. Spectral dependencies

To discriminate the defect level spectra we have investigated the photocurrent dependencies on the quantum energy of the exciting light. These dependencies at low and at the room temperatures are presented in Fig. 3. At both temperatures a clear maximum is seen, the increase of which starts at about 2.75 eV. This maximum is related to the band to band generation. A drop that takes place at the higher energy side could be associated with the increasing absorption and, as a consequence, growing influence of the surface recombination. Other features at the room temperature are masked by the high conductivity of the samples. The most interesting results related to the defect bands appear at low temperature in the region between 1 eV and 2.5 eV. It is necessary to note that these results were not always repeatable in details in subsequent measurements, but they had demonstrated qualitative coincidence. From the spectral dependencies of photocurrent several defect-related maxima in the region between 1 eV and 2.5 eV were identified, being dependent on the sample prehistory. All the curves in Fig. 3 except 3 were measured starting

from the low quantum energies. The measurement directions are indicated by the arrows. Curve 1 was obtained after relaxation of the sample in the dark for 20 hours without applied voltage. Meanwhile curves 2 and 3 were obtained after keeping the sample with applied 60 V voltage at the room temperature for 6 hours, afterwards cooling it down and scanning the spectra in different directions.

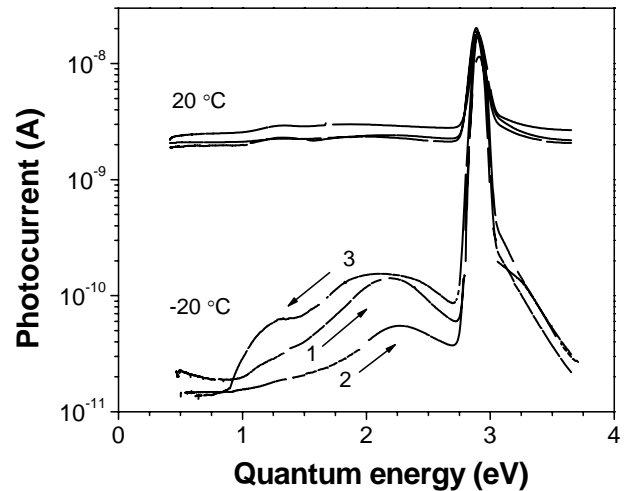


Fig. 3. Photocurrent spectral dependencies at different temperatures. The measurement directions are indicated by the arrows

Maximum at about 1.2 eV used to appear if the spectra were scanned from the high to the low quantum energies. Meanwhile the height of the maximum at about 2.1 eV–2.2 eV used to decrease if the sample was kept biased for several hours. In Fig. 3 two different effects are seen. First of all, the not always reproducible fatigue effect could be introduced by the applied voltage, that resulted in the reduction of the amplitude of the defect band with the maximum at about 2.1 eV–2.2 eV. On the other hand, if the spectra were scanned from the high energy side, this resulted in the appearance of the second band with the maximum located at about 1.2 eV. Similar complicated defect structure was also revealed by PL in [7]. The luminescence in the range 1.5 eV–2.0 eV was observed under X-ray excitation and was ascribed to the diffusion-controlled recombination in [7], meanwhile PL at 1.1 eV was observed in the short-lived absorption spectra under pulsed electron beam excitation in [8] and it was explained to be due to the a hole trapped at cation vacancy ($Tl^{2+}Vc^-$). This centre can be created if hole is trapped by a pre-irradiation vacancy, as well as result from the radiation-induced Frenkel pair formation ($Tl^{2+}Vc^-$ and interstitial thallium atom Tl_i^0). Our results indicate that such vacancy can also be light-induced, even though the intensity of light, passing through the monochromator, is low. Therefore we have investigated transient effects under the light illumination and in the dark at different temperatures.

3.3. Transient photocurrent kinetics

Kinetics of the photocurrent were measured at different temperatures upon the excitation of the sample by the light with the wavelength from the maximum absorption region.

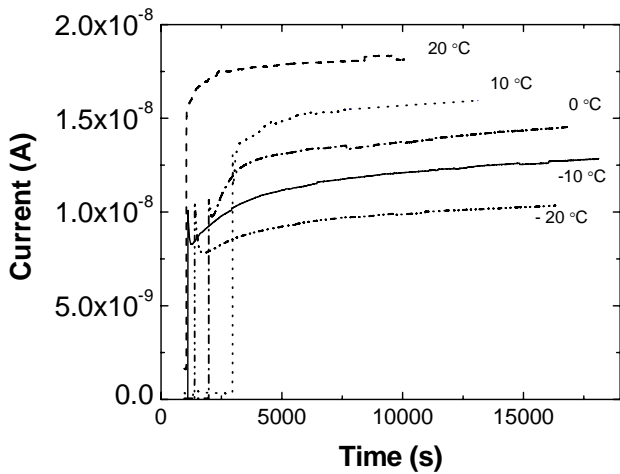


Fig. 4. Current transients measured at different temperatures, after the onset of the light excitation corresponding to the photoconductivity maximum. Curves are shifted in time for the sake of convenience

In Fig. 4 examples of such kinetics are shown, that represent most general and repeatable tendencies. The best expressed feature is the presence of two different trends in the photocurrent kinetics. When the light is switched on, after the sharp current jump, current decrease takes place, which later on is replaced by its growth until the saturation is reached. All these processes are thermally activated. At 20 °C current decrease was no longer observed experimentally in some cases. Nevertheless, as it was already mentioned, the results were not repeatable in detail as it is demonstrated in Fig. 5.

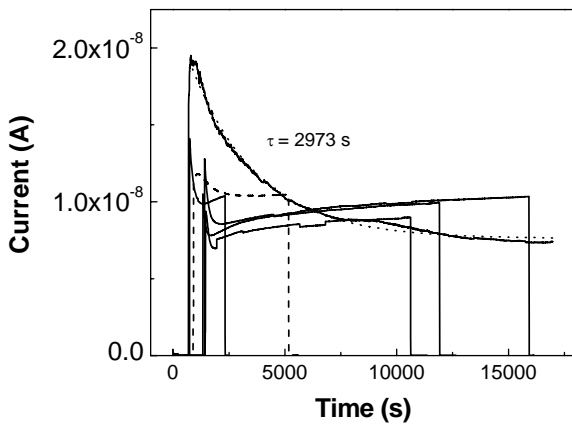


Fig. 5. Series of current transients measured at -20 °C after the onset of the light excitation corresponding to the photoconductivity maximum. Curves are shifted in time for the sake of convenience

In most cases, independent on the previous excitation, current kinetics demonstrated the mentioned minimum with very similar relaxation times. But, in few cases at low temperature we have observed well expressed current decrease with very long relaxation time of about 3000 s without its subsequent growth, as it demonstrated by the curve in Fig. 5 with nearby indicated evaluated relaxation time constant. This trace was observed after several days of relaxation of the sample at the room temperature without applied voltage. Nevertheless later we did not succeed in repeating such behaviour. Though the dashed curve in the same Figure, which was measured after the same relaxation time, also demonstrated significantly longer

decay time, but its drop was not so well expressed as that of the black curve. It is necessary to note that both processes could be approximated well by the exponential dependencies with single characteristic time constants. Therefore, to evaluate thermal activation behaviour of these two processes, we have calculated the averages of both characteristic time constants from many measurements. The results are presented in Fig. 6.

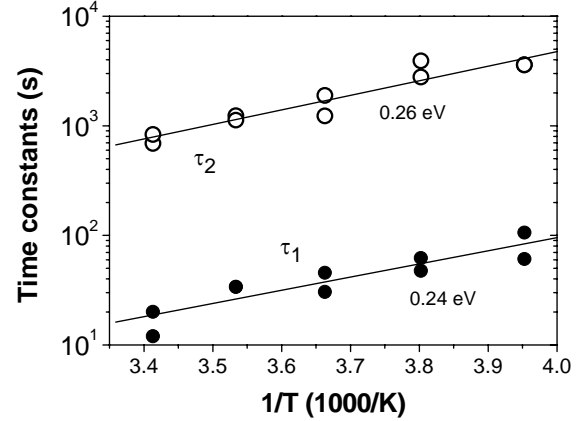


Fig. 6. Dependence of the averaged time constants τ_1 and τ_2 , describing current decrease and the following growth, respectively

It can be seen that the averaged time constants of current decay and its following growth differ by about two orders of magnitude and, within the range of accuracy, have the same thermal activation energy values of about 0.24 eV–0.27 eV. Therefore, it could be supposed that the total photocurrent kinetics could be caused either by two different competitive processes or by a single complex process. The first possibility is supported by the presence of two different current trends as described earlier. In that case the current decrease could be probably ascribed to the faster electronic process because of the trapping and/or recombination of light-generated carriers to the defect centres associated with potential inhomogeneities. This process could be similar to the known mechanism of the thermal quenching. The following current increase might be attributed to the growing ionic conductivity caused by TI^+ ions, as it was observed in [6]. Nevertheless the similar thermal activation energy values of both characteristic time constants indicate that probably they could be attributed to the single process. Similar non-monotonous behaviour is characteristic for the diffusion from a limited material source [5]. In such case the total number of extraneous atoms at a certain point is given by:

$$N = \frac{A}{\sqrt{t}} \exp\left(-\frac{B}{t}\right). \quad (1)$$

Here A and B are the diffusion- and material-related constants.

A model curve calculated according to Eq. (1) is presented in Fig. 7. It can be seen that this curve qualitatively demonstrates inverse dependence in time as compared to the experimental traces. Therefore, if one assumes that transport properties are given by carrier and/or ion mobility that are limited by a varying number of scattering centres, then at least qualitative coincidence could be obtained, if mobility is supposed to demonstrate the

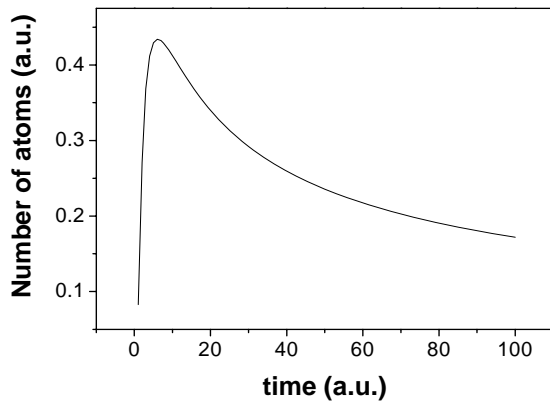


Fig. 7. Model curve calculated according to Eq. (1), representing number of extraneous atoms diffusing from a limited source at a certain space point depending on time.

inverse proportionality to the number of scattering centres: $\mu = 1/N$. Similar kinetic effects, just less expressed, were also observed without light excitation. The signal was much smaller, and consequently, in many cases distorted by the already mentioned noise effects, especially at low temperatures. Therefore we could not make any definite quantitative evaluations. At 20 °C temperature the already described current growth was observed after switching on the bias. Nevertheless at lower temperatures only current decrease took place without any indications of its further growth, at least within the experiment duration of up to 2×10^4 s. This is in contrast to the described behaviour observed with light excitation. The characteristic time constants were much longer as well. Notably that the very fast initial current drop with no kinetics and residual effects took place at the moments when the bias was switched off.

4. SUMMARY AND CONCLUSIONS

We have investigated photoelectrical and current transient properties of TlBr in the temperature region from -20 °C up to $+20$ °C, in which the effect of ionic conductivity changes significantly. Samples were provided with the evaporated gold contacts. In order to prevent the long-living sample polarization, low applied electric fields of less than 150 V/cm were used. In this region the current-voltage dependencies were linear, and the sample conductivities at 20 °C were about $(3-4) \times 10^{10} \Omega^{-1} \text{cm}^{-1}$. The evaluated thermal activation energy value of conductivity of about 0.78 eV could stand for several mechanisms, e. g., electronic and ionic conductivity. From the spectral dependencies of photocurrent several defect-related maxima in the region between 1 eV and 2.5 eV were identified, being dependent on the sample prehistory. Maximum at about 1.2 eV have appeared if the spectra were scanned from the high to the low quantum energies. Meanwhile the height of the maximum at about 2.1 eV–2.2 eV used to

decrease if the sample was kept biased for several hours. The transient photocurrent kinetics have demonstrated a complicated structure: when the light was switched on, the photocurrent, after its sharp initial jump, used to decrease demonstrating a minimum that again was followed by the current growth until the saturation was reached. Such complex behaviour could be explained either by the combined trapping and/or recombination of light-generated carriers to the defect centres associated with potential inhomogeneities, followed by the growing ionic conduction or by the variation in time of the ion diffusion-related scattering. The evaluated thermal activation energy of the time constants of both processes was found to be 0.24 eV–0.27 eV. The obtained results indicate that ionic conductivity can take place also at -20 °C, though its influence is less because of the thermally activated character. This is in contrast to the results proposed in [1], that in TlBr radiation detectors at -20 °C no degradation was observed. Moreover our results indicate that even light excitation with low intensity from the maximum absorption band might be effective in capacitating ionic conductivity.

REFERENCES

1. **Sellin, P. J.** Recent Advances in Compound Semiconductor Radiation Detectors *Nuclear Instruments and Methods in Physics Research Section A* 513 2003: pp. 332 – 339.
2. **Hitomi, K., Matsumoto, M., Muroi, O., Shoji, T., Hirate, Y.** Thallium Bromide Optical and Radiation Detectors for X-ray and Gamma-ray Spectroscopy *IEEE Transactions on Nuclear Science* 49 (5) 2002: pp. 2526 – 2529.
3. **Hitomi, K., Matsumoto, M., Muroi, O., Shoji, T., Hirate, Y.** Characterization of Thallium Bromide Crystals for Radiation Detector Applications *Journal of Crystal Growth* 225 2001: pp. 129 – 133.
4. **Onodera, T., Hitomi, K., Shoji, T.** Spectroscopic Performance and Long-term Stability of Thallium Bromide Radiation Detectors *Nuclear Instruments and Methods in Physics Research Section A* 568 2006: pp. 433 – 436.
5. **Pavlov, P. V., Khohlov, A. V.** Solid State Physics. High School, Moscow, 1985 (in Russian).
6. **Vaitkus, J., Banys, J., Gostilo, V., Zatuloka, S., Mekys, A., Storasta, J., Žindulis, A.** Influence of Electronic and Ionic Processes on Electrical Properties of TlBr Crystals *Nuclear Instruments and Methods in Physics Research Section A* 546 2005: pp. 188 – 191.
7. **Grigorjeva, L., Millers, D.** The Model of Recombination Process in TlBr *Nuclear Instruments and Methods in Physics Research Section B* 191 2002: pp. 131 – 134.
8. **Grigorjeva, L., Millers, D.** Excitonic Processes in Thallous Halides Excited by electron Beam *Electrochemical Society Proceedings* 25 1998: pp. 438 – 443.

DOI: 10.5755/j02.ms.26238